An ab initio study of crystal field effects, part 3: Solid- and gas-phase geometry of formamide, modeling the changes in a peptide group due to hydrogen bonds

ARTICLE *in* STRUCTURAL CHEMISTRY · DECEMBER 1990

Impact Factor: 1.84 · DOI: 10.1007/BF00673483

4 AUTHORS, INCLUDING:

Paul L A Popelier
The University of Manchester
190 PUBLICATIONS **7,115** CITATIONS
SEE PROFILE

Christian Van Alsenoy
University of Antwerp
403 PUBLICATIONS **5,927** CITATIONS
SEE PROFILE

Struct. Chem., Vol. 2, pp. 3–9. ISSN 1040-0400

An Ab Initio Study of Crystal Field Effects, Part 31: Solid- and Gas-Phase Geometry of Formamide, Modeling the Changes in a Peptide Group Due to Hydrogen Bonds

*P. Popelier, A. T. H. Lenstra, C. Van Alsenoy, and H. J. Geise**
University of Antwerp (UIA), Department of Chemistry, B-2610 Wilrijk, Belgium

A model of the solid state of formamide is constructed by optimizing a central molecule in an electrostatic field of the proper symmetry. Attention is paid to the way the electrostatic charges are obtained. Point charges obtained from a Mulliken population analysis yield a final set of atomic charges in the central molecule that agree reasonably well with those obtained experimentally after a κ-refinement of formamide. Point charges from a so-called stockholder partitioning agree slightly less. Furthermore, the simple crystal field adaptation of standard ab initio methods reproduces within experimental limits the differences in C=O and C—N lengths, observed between the gas-phase and the solid state geometry. Again, a Mulliken field agrees slightly better than a stockholder field, but the difference in performance is statistically insignificant. In a survey of 221 high-quality single-crystal x-ray determinations of compounds containing the peptide group N—C=O, we found evidence supporting quantitatively the conclusion that the increase of C=O and the decrease of C—N bond length in the gas-to-solid transition is dominated by the effects of hydrogen bonding. It was shown that the C=O bond lengthens by about 0.011 Å per H-bond it accepts, while the N—C bond diminishes by about 0.015 Å per H-bond it donates.

INTRODUCTION

A molecule in the solid phase often has a geometry slightly different from the one in the gaseous phase, particularly when intermolecular hydrogen bonds are present. A theoretical technique that gives such differences reliably would be most welcome. A method based on the incorporation of a simple electrostatic crystal field model of the solid state into standard ab initio calculations has attracted increasing interest [1–6]. It is computationally inexpensive and has been successfully applied, e.g., in the conformational analysis of cyanoformamide [3], cyanamide [4], and acetamide [5]. A number of methodological aspects, however, have not yet been investigated. One of them, namely, the influence of the manner in which the electrostatic crystal field charges are computed, is addressed in this work. Formamide is taken as the test molecule, because it is one of the very few molecules for which the geometry differences in going from the gaseous to the crystalline state have been determined with sufficient accuracy. Furthermore, it is the simplest model compound containing a peptide unit engaged in hydrogen bonding. Therefore, another aim of this work is to investigate the response of the peptide geometry to hydrogen bonding conditions.

Kitano and Kuchitsu analyzed the molecular structure of formamide in the gas phase by electron diffraction [7]. Stevens determined the structure as well as the electron density distribution in the solid from low-temperature, high-order x-ray data [8]. The molecule is within experimental accuracy planar in both phases, but the C=O bond is 0.027(5) Å longer and the C—N bond 0.042(5) shorter in the crystal. We will show that the crystal field approach reproduces the geometric features and the experimental atomic charges satisfactorily. Finally, a statistical analysis is per-

†Part 2, see Ref. [5].
*To whom correspondence should be addressed.

Manuscript received 11/13/89; accepted 4/18/90.

1040-0400/91/$3.50 + .25

Table 1. Experimental and Calculated Geometries of Formamide in the Gaseous and Solid State[a]

	Gas-Phase r_g geometry		Solid state r_0^α geometry			Differences Δ		
			Mulliken	stockholder		Exp.	Mulliken	stockholder
	Calc[b]	Exp[c]	Calc[b]	Calc[b]	Exp[d]	Col. 2–Col. 5	Col. 1–Col. 3	Col. 1–Col. 4
C=O	1.215	1.212(3)	1.245	1.227	1.239(4)	−0.027(5)	−0.030	−0.012
C—N	1.376	1.368(3)	1.343	1.356	1.326(4)	+0.042(5)	+0.033	+0.020
N—H_1	1.025	1.027(6)	1.032	1.022	1.01(5)	+0.02(5)	−0.01	+0.00
N—H_2	1.023	1.027(6)	1.032	1.024	1.01(5)	+0.02(5)	−0.01	+0.00
C—H	1.117	1.125(12)	1.107	1.107	1.09(5)	+0.04(4)	+0.01	+0.01
N—C=O	125.1	125.0(4)	126.8	125.7	124.9(3)	+0.1(5)	−1.7	−0.6
	Col. 1	Col. 2	Col. 3	Col. 4	Col. 5			

[a]Distances in Å, angles in decimal degrees. See Figure 1 for atomic numbering. Estimated standard deviations in parentheses.
[b]Distances are transformed using $r_g(\text{calc}) = r(\text{4-21G}) + \delta$ and $r^0_\alpha(\text{calc}) = r(\text{4-21G}) + \delta - K$, with δ(C=O) = 0.000Å, δ(C—N) = 0.020 Å, δ(C—H) = 0.034 Å, δ(N—H) = 0.031Å, K(C=O) = 0.004 Å, K(C—N) = 0.007 Å, K(C—H) = 0.010 Å. No corrections are applied to valence angles.
[c]Taken from ref. [7], combined electron diffraction-microwave model. N—H_1 is kept equal to N—H_2, and the molecule is assumed planar.
[d]Taken from ref. [8].

formed on 221 CONH-containing compounds determined by single-crystal x-ray analysis of which the results strongly support the theoretical approach.

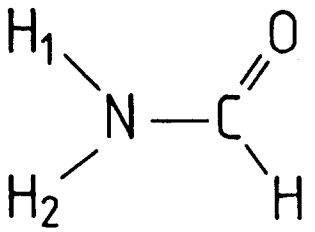

Figure 1. Atomic numbering scheme. H_1 is sometimes referred to as H(*trans*) and H_2 as H(*cis*) [18].

CALCULATIONS

Equilibrium geometries of formamide were enumerated using Pulay's gradient method, Pulay's computer program TEXAS [9–11], the 4-21G basis set [12], and full, unconstrained geometry optimizations. The choice of the basis set was dictated despite its shortcomings, because it is the only basis set for which a set of conversion factors is available to convert the r(4-21G) geometry into an r_g geometry (see Discussion and Comparison with Experiment below). Relaxation was considered complete when the largest residual force on any atom had dropped below 10 pN. It is believed [13] that at this level of refinement bond lengths are within 0.0005 Å and valence angles within 0.2° of the 4-21G optimum value. In Table 1 (Gas phase section) we give only the data directly relevant to the problems at hand. For a review of previous theoretical work on the geometry of free formamide, including an extensive study of basis set effects, see [14] and [15].

To estimate the influence of neighboring molecules on the optimized geometry of a central molecule, we represent the neighbors by a series of electrostatic point charges. These point charges are put at atomic positions given by, e.g., x-ray experiment to ensure the correct symmetry of the crystal field. In other words, the x-ray experiment provides an external geometry, i.e., the center of mass position and the Eulerian angles of the central and surrounding molecules with respect to the crystallographic system of axes. The external geometry is fixed, at least in this work, whereas the internal geometry (3N-6 parameters, representing bond lengths, valence, and torsion angles) remains refinable. Subsequently, the influence of the electrostatic crystal field on the central molecule is calculated by standard ab initio methods and the resulting new internal parameters of geometry and charges are fed back into the calculations until convergence is reached.

Starting from the converged 4-21G model of the free molecule as the central molecule, two series of solid state calculations were performed, one in which the atomic charges on the neighboring molecules were enumerated from a Mulliken population analysis [16] and the other in which the charges were derived from a so-called stockholder partitioning [17] (see Discussions and Comparison with Experiment, below). In each series the charges were put on sites to give a monoclinic environment of $P2_1/n$ symmetry (the space group of formamide [8]). The number of molecules building up the crystal field was 162 (i.e., a total of 6 × 162 = 972 point charges in a sphere with radius 11Å). In previous investigations we had found that such a spherical cluster of surrounding molecules is suffi-

Table 2. Comparison of Net Atomic Charges (e) from Mulliken Analysis, Stockholder Partitioning, and from an Experimental κ Determination

	O	N	C	$H_1(N)$	$H_2(N)$	H(C)
Mulliken						
Start[a]	−0.65	−0.93	0.66	0.37	0.38	0.17
Final[b]	−0.82	−0.96	0.66	0.46	0.45	0.21
Stockholder						
Start[a]	−0.35	−0.17	0.22	0.13	0.13	0.04
Final[b]	−0.42	−0.16	0.22	0.16	0.15	0.05
Experiment[c]	−0.55(4)	−0.78(7)	0.51(8)	0.39(3)	0.40(3)	0.03(3)

[a]Start values in solid state computations are those of the converged free molecule (gas phase).
[b]Final values of solid state after convergence has been reached in forces.
[c]Estimated standard deviations in parentheses.

ciently large [5,6]. The refinements were continued until convergence was reached again (largest residual force smaller than 10 pN). The results are presented in Table 1, Solid state section.

DISCUSSION AND COMPARISON WITH EXPERIMENT

The quality of an electrostatic crystal field model will obviously depend on the quality of the point charge values, and therefore two series of solid state calculations were performed. In the first series the well-known Mulliken population analysis was employed in which atomic charges Q(i) are obtained by addition of the appropriate products of density matrix and overlap matrix elements [16]. The advantage is the operational simplicity, while the disadvantage is that the resulting charges are somewhat arbitrary and strongly basis-set–dependent. In the second series the less-common "stockholder" partitioning was used in which the charges Q(i) are calculated by [17]:

$$Q(i) = -\frac{\rho(i)}{\sum_i \rho(i)}\,\rho(\text{mol})\text{dv}$$

ρ(mol) represents the molecular electron density and $\Sigma\rho$(i) the electron density of a (hypothetical) assembly of isolated spherical atoms placed at the nuclear positions. The latter is sometimes called a "promolecule." The attraction of the partitioning scheme is that it not only allows to approach the Q(i) by quantum-chemical computations but also experimentally. The electron density of the promolecule is accessible through a molecular model obtained from a neutron diffraction or a high-order x-ray determination, while the molecular density is accessible through a multipole refinement. In this work, however, ρ(mol) and $\Sigma\rho$(i) were computed using the 4-21 G basis set.

The Q(i) values during the solid state calculations are summarized in Table 2. This table clearly shows that the change from the free molecule (start cycle) to the molecule in the solid state (final cycle) produces changes in the net atomic charges. They are most pronounced for the atoms (H_1, H_2, and O) directly involved in the hydrogen bonding. The calculated Q-values are then to be compared to the experimental ones obtained in a profound study by Stevens [8] after a κ-refinement (for a discussion of the method see, e.g., Coppens [19]). The agreement between the Mulliken Q-values and the experimental ones is satisfactory, particularly if one realizes that κ-derived Q-values by their nature are approximate and their estimated standard deviations (esd's) probably underestimated [20,21].

Turning our attention to geometries, one has to remember that physically meaningful comparisons between ab initio calculated geometric parameters and experimental ones can only be made if both are brought to the same geometrical basis. The calculations give a r(4-21G) geometry, to be interpreted as internuclear distances of a nonvibrating molecule, subject to the approximations of the 4-21G basis. On the other hand, all experimental values include effects of molecular vibrations, the exact manner depending on the experimental method and conditions employed. For free molecules the conversion is well documented [22–25], particularly for r_g-type distances that can be derived from gas-phase electron diffraction data. The r(4-21G) geometry is converted to internuclear distances of r_g-type by

$$r_g(\text{calc}) = r(4 - 21\text{G}) + \delta$$

where δ is an empirical correction depending on the type of bond concerned as well as on the basis set. For the solid state the situation is somewhat more complicated. Parameters from standard single-crystal x-ray determinations are less suitable, because they are based on distances between the centers of electron densities and not on internuclear distances. The latter may be obtained from neutron diffraction analysis and high-order x-ray refinements, which after correction for thermal translational and rotational effects will ap-

Table 3. Some Differences in Geometry Between a Molecule in the Gas Phase and in the Solid State[a]

	C=O		C—N		N—C=O		
	Δ(calc)	Δ(exp)	Δ(calc)	Δ(exp)	Δ(calc)	Δ(exp)	Ref.
Formamide	0.030	0.027(5)	−0.033	−0.042(5)	1.7	−0.1(5)	This work
Acetamide	0.022	0.030(4)	−0.021	−0.043(4)	0.2	0.3(6)	[5]
Cyanoformamide	0.012	0.026(2)	−0.017	−0.034(2)	2.3	2.2(4)	[3]

[a] Δ = solid state r^0_α geometry value − gas-phase r_g geometry value. Δ(calc.) is obtained using Mulliken population analysis. Distances in Å, angles in decimal degrees, estimated standard deviation in parentheses.

proach r^0_α geometry. That is a geometry based on averaged nuclear coordinates of the molecule in the vibrational ground state. Ab initio distances are brought to r^0_α basis by

$$r^0_\alpha(\text{calc}) = r(\text{4-21G}) + \delta - K$$

where δ is defined as above and K is the contribution of the vibration perpendicular to the bond. These K-values can be calculated from normal coordinates using a harmonic force field [25–29], but their applicability in the solid state has not yet been rigorously established. We estimate the combined uncertainty connected to the use of K and δ in solid state calculations to be 0.01 Å.

Table 1 lists the 4-21G calculated geometry for the isolated and the solid state molecule brought to r_g and r^0_α basis, respectively, together with the δ and K values used. The agreement between the calculated gas phase geometry and the experimental r_g-geometry [7] is excellent. The maximum discrepancy, occurring in the C—N bond length, is about twice the experimental esd.

In addition, the direct comparison between calculated and experimental solid state geometry shows no discrepancies outside the expected limits. The most gratifying result, however, is that the differences Δ (defined as Δ = solid state value − gas-phase value) show good agreement for the well-established C=O and C—N bond lengths, while for none of the other parameters the Δ-value is outside the (large) error limits. It may be noted that the atomic charges obtained in the Mulliken analysis perform slightly better than those obtained by stockholder partitioning. However, the difference in performance is statistically not significant. We conclude, therefore, that the choice of atomic charges is not very critical when we want to enumerate the geometrical consequences on the molecular level of a gas-to-solid phase transition. Differences Δ between gas-phase and solid state geometries of peptide sequence O=C—N are now available for formamide, acetamide, and cyanoformamide. The data presented in Table 3 show a good agreement between Δ(exp) and Δ(calc), proving the applicability of the crystal field approach. The data also show the experimental values (Δ(C=O) and Δ(C—N) to be quasiconstant. This points to hydrogen bonding as the cause of the geometry differences, a conclusion in agreement with previous authors [30,31]. The variation in the N—C=O valence angle seems to be governed primarily by other factors than H-bonding.

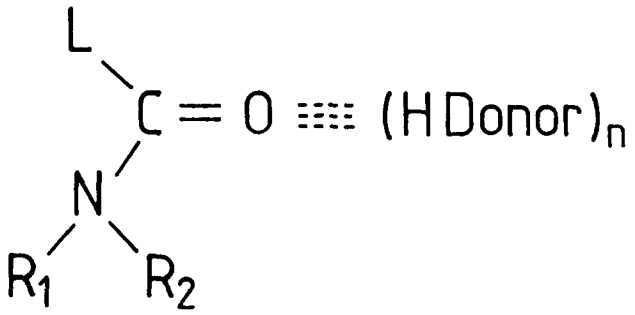

Figure 2. Search unit in the Cambridge Crystallographic Data Base [32].

O=C—N Geometry and Hydrogen Bonding

The influence of hydrogen bonding on the peptide geometry is further investigated using the Cambridge Crystallographic Data Base [32]. The data base was searched for the structural unit depicted in Figure 2, excluding metal-containing complexes and excluding compounds containing oxygen or sulfur at L, the atom directly bonded to the carbonyl carbon. Furthermore, room temperature studies and determinations resulting in an R-value above 0.05 as well as disordered structures and structures with protonated C=O bonds were rejected. The examination included a search for three (n = 3), two (n = 2), one (n = 1), and no (n = 0) hydrogen bonds to C=O, the donor being either nitrogen, oxygen, fluorine, or sulfur. Finally, it proved necessary to specify a hydrogen bond by restricting the donor(D)—acceptor(A) distance and D—H—A angle to the ranges 2.3 Å ≤ D———A ≤ 3.1 Å and 130° ≤ D—H———A ≤ 185°, respectively. The number of hits for the four groups (n = 0, 1, 2, 3) and the averages of the C=O, C—N bond length, and O=C—N angle are shown in Table 4. A survey of the data shows that

Table 4. Survey of Statistical Analysis of the System $R_1R_2N—C(L)O—(H\ Donor)_n$[a], in Function of Number of H-bonds donated (n)

	$n = 0$	$n = 1$	$n = 2$	$n = 3$
No. of structures found	131	64	16	10
Average C=O length (Å)	1.226	1.234	1.247	1.259
Average C—N length (Å)	1.363	1.346	1.343	1.341
Average O=C—N angle (°)	122.8	123.0	122.4	121.3

Results of linear regression analysis: parameter = $a + bn$

	C=O	C—N	O=C—N
Intercept (a)	1.225	1.359	123.1
Slope (b)	0.011	−0.007	−0.5
Correlation coefficient	0.995	0.89	0.87

[a]The list of compounds used is available (1 page) as supplementary material. Ordering information is given on any current masthead page.

Table 5. Distribution of Crystal Structures in the 12 Subclasses of the $R_1R_2NC(L)O—(H\ Donor)_n$ System, and Averages of C=O, C—N (in Å) Bond Lengths and O=C—N Angle (Degrees), with estimated standard deviations in parentheses.

	$n = 0$	$n = 1$	$n = 2$	$n = 3$
No. crystal structures				
R_1 and $R_2 \neq H$	86	4	0	0
$R_1 = H$; $R_2 \neq H$	42	56	6	0
$R_1 = R_2 = H$	3	4	10	10
Average C=O length				
R_1 and $R_2 \neq H$	1.225(1)	1.230(1)	—	—
$R_1 = H$; $R_2 \neq H$	1.228(2)	1.234(1)	1.245(5)	—
$R_1 = R_2 = H$	1.235(2)	1.242(1)	1.248(4)	1.259(1)
Average C—N length				
R_1 and $R_2 \neq H$	1.367(3)	1.369(7)	—	—
$R_1 = H$; $R_2 \neq H$	1.357(4)	1.346(2)	1.352(7)	—
$R_1 = R_2 = H$	1.341(15)	1.327(3)	1.338(5)	1.341(2)
Average O=C—N angle				
R_1 and $R_2 \neq H$	122.9(3)	121.8(5)	—	—
$R_1 = H$; $R_2 \neq H$	122.6(2)	123.1(3)	121.9(5)	—
$R_1 = R_2 = H$	122.3(9)	123.0(1)	122.7(4)	121.3(3)

Bivariate regression analysis[a]: parameter = $a + bn + cm$

	C=O	C—N	N—C=O
a	1.223	1.368	122.6
b	0.008	0.0002	−0.4
c	0.006	−0.016	0.2
Correlation Coefficient	0.991	0.934	0.607

[a]n = number of H-bonds accepted by C=O; m number of hydrogen (—H) atoms attached to peptide-N.

the C=O bond excellently fits to

$$\text{CO length (Å)} = 1.225 + 0.011n$$

where n is the number of H-bonds the C=O accepts. The linear correlation coefficient is $r = 0.995$. Comparing the increase in C=O length per accepted H-bond (slope b = 0.011Å) with the Δ-values given in Table 3 one sees a good agreement, by realizing that in the crystal structures of formamide and acetamide each C=O group accepts two hydrogen bonds, whereas in cyanoformamide the C=O group accepts only one H-bond.

In an analogous fashion, we find each time the C=O end of the peptide group accepts an H-bond, the CN bond decreases by 0.007 Å and the N—C=O angle by 0.5°. The correlation coefficients, however, are considerably lower (see Table 4) and only semi-quantitative agreement exists between b(CN) and Δ(CN) (see Table 3). No agreement exists between b(N—C=O) and the values of Δ(N—C=O) given in Table 3. Two

Table 6. Analysis of C—N Data Set After Rearrangement into a System Typified as $OC—NH_m\cdots O{=}C—$ / $O{=}C—$

	$m = 0$	$m = 1$	$m = 2$
No. of structures	90	104	27
Average C—N length	1.367	1.351	1.338

possible causes come to mind. First, different substituents on nitrogen as well as various substituents L (see Figure 2) may also cause a change in C—N length. Second, differences in L have more influence on the N—C=O angle than the number of H-bonds accepted by the C=O group. We examined these possibilities by subdividing each of the four groups (n = 0, 1, 2, 3) into three classes.

1. Two hydrogens attached to the peptide nitrogen ($R_1 = R_2 = H$),
2. One hydrogen on the peptide nitrogen ($R_1 = H$; $R_2 \neq H$),
3. No hydrogen on peptide nitrogen (R_1 and $R_2 \neq H$)

Table 5 summarizes the statistical results together with those of a bivariate linear regression analysis. The bivariate approach of C=O is no improvement over the univariate, a result in line with the idea that the C=O length is dominated primarily by n, the number of H-bonds it accepts. In contrast, the bivariate approach to C—N performs significantly better than the univariate. In fact, it even suggests that the C—N length is solely dependent on m, the number of —H atoms attached to the peptide-N. If we now interpret m as the number of H-bonds the peptide-N can *donate*, rearrange the C—N data set accordingly (Table 6), and perform a new regression on m we obtain

$$CN = 1.367 - 0.015\ m$$

Knowing that in formamide the NH_2 group donates two H-bonds, this result [b(CN) = −0.015 Å per H-bond *donated*], agrees very well with the corresponding Δ(CN) given in Table 3. Finally, we note a bad correlation between the N—C=O angles (see Table 5) on the one hand and n and m on the other. This result is to be expected when factors other than H-bonds dominate the N—C=O angle.

ACKNOWLEDGMENTS

The help of Mr. H. Bruning (Technical University Twente, The Netherlands), who programmed the stockholder partitioning routine, is gratefully acknowledged.

CVA acknowledges support as a Research Fellow by the Belgian National Science Foundation, NFWO. This work was partly supported by North Atlantic Treaty Organization (NATO), Research Grant Number 0409/88. The text presents in part results of the Belgian Program on Interuniversity Attraction Poles initiated by the Belgian State—the Prime Minister's Office, Science Policy Programming. The scientific responsibility, however, remains with the authors.

REFERENCES

1. Almlöf, J.; Kvick, A.; Thomas, J. O. *J. Chem. Phys.*, **1973,** *59*, 3901.
2. Almlöf, J.; Wahlgren, U. *Theor. Chim. Acta,* **1973,** *28*, 161.
3. Saebo, S.; Klewe, B.; Samdal, S. *Chem. Phys. Lett.*, **1983,** *97*, 499.
4. Helgaker, T. U.; Klewe, B. *Acta. Chim. Scand.*, **1988,** *A42*, 269.
5. Popelier, P.; Lenstra, A. T. H.; Van Alsenoy, C.; Geise, H. J. *J. Am. Chem. Soc.*, **1989,** *111*, 5658.
6. Popelier, P.; Lenstra, A. T. H., Van Alsenoy, C.; Geise, H. J. *Acta Chem. Scand.*, **1988,** *A42*, 539.
7. Kitano, M.; Kuchitsu, K. *Bull. Chem. Soc. Jpn.* **1974,** *47*, 67.
8. Stevens, E. D. *Acta Crystallogr.*, **1978,** *B34*, 544.
9. Pulay, P. *Mol. Phys.*, **1969,** *17*, 197.
10. Pulay, P. *Theor. Chim. Acta.*, **1979,** *50*, 299.
11. Pulay, P. In *Modern Theoretical Chemistry;* Schäfer III, H. F. Ed.; Plenum Press: New York; 1977; Vol. 4, p. 154.
12. Pulay, P.; Fogarasi, G.; Pang, F.; Boggs, J. E. *J. Am. Chem. Soc.*, **1979,** *101*, 2550.
13. Schäfer, L. *J. Mol. Struct.*, **1983,** *100*, 1.
14. Carlsen, N. R.; Radom, L.; Riggs, N. V.; Rodwell, W. R. *J. Am. Chem. Soc.*, **1979,** *101*, 2233.
15. Wright, G. M.; Simmonds, R. J.; Parry, D. E. *J. Comp. Chem.*, **1988,** *9*, 600.
16. Mulliken, R. S. *J. Chem. Phys.*, **1955,** *23*, 1833, 2333, 2338.
17. Hirschfeld, F. L. *Theor. Chim. Acta,* **1977,** *44*, 129.
18. Berthod, H.; Pullman, A.; Hinton, J.; Harpool, D. *Theor. Chim. Acta,* **1980,** *57*, 63.
19. Coppens, P. In *Electron Distributions and the Chemical Bond,* Coppens, P.; Hall, M. B., Eds.; Plenum Press: New York, **1982;** pp. 61–92.
20. Downs, J. W.; Hill, R. J.; Newton, M. D.; Tossel, J. A.; Gibbs, G. V. In *Electron Distributions and the Chemical Bond,* Coppens, P., Hall, M. B., Eds.; Plenum Press: New York, **1982;** pp. 173–189.
21. Lenstra, A. T. H.; De Wolf, M.; Vanhouteghem, F. *Bull. Soc. Chim. Belg.*, **1985,** *94*, 697.
22. Kuchitsu, K. In *Molecular Structure and Vibrations;* Cyvin, S. J., Ed.; Elsevier: Amsterdam, **1972;** Chapter 12.
23. Klimkowski, V. J.; Ewbank, J. D.; Van Alsenoy, C., Scarsdale, J. N.; Schäfer, L. *J. Am. Chem. Soc.*, **1982,** *104*, 1476.
24. Van Alsenoy, C.; Klimkowski, V. J.; Schäfer, L. *J. Mol. Struct. Theochem.*, **1984,** *109*, 321.
25. Geise, H., Pyckhout, W. In *Stereochemical Applications of Gas Phase Electron Diffraction;* Hargittai, I.; Hargittai, M. Eds.; VCH Publishers: New York, **1989,** Part A, Ch. 10.

26. Cyvin, S. J. In *Molecular Vibrations and Mean-Square Amplitudes*. Oslo Universitetsforlaget: Oslo, Norway, **1968,** Ch. 7.
27. Sellers, H. L.; Schäfer, L. *J. Mol. Struct.*, **1979,** *51*, 117.
28. Gwinn, W. D. *J. Chem. Phys.*, **1971,** *55*, 477.
29. Stolevik, W. D.; Seip, H. M.; Cyvin, S. J. *Chem. Phys. Lett.*, **1972,** *15*, 26.
30. Robin, M. B.; Bovey, F. A.; Basch, H. In *The Chemistry of the Amides;* Zabicky, J., Ed.; Wiley-Interscience: New York, **1970;** pp. 3.
31. Beagly, B. In *Molecular Structure by Diffraction Methods;* Chemical Society Specialist Periodical Report, Sim, G. A.; Sutton, L. E.; Eds.; The Chemical Society: London, **1975;** Vol. 3, pp. 66.
32. Allen, F. H.; Bellard, S.; Brice, M. D.; Cartwright, B. A.; Doubleday, A.; Higgs, H.; Hummelink, T.; Hummelink-Peeters, B. G.; Kennard, O.; Motherwell, W. S. D.; Rodgers, J. R.; Watson, D. G. Acta Crystallogr **1979,** *B35*, 233.